Astronomy & Astrophysics manuscript no. aa3779-05
January 6, 2006

SOHO/CDS observations of waves above the network

P. Gömöry[1,2], J. Rybák[1], A. Kučera[1], W. Curdt[3], and H. Wöhl[4]

[1] Astronomical Institute of the Slovak Academy of Sciences, 05960 Tatranská Lomnica, Slovakia
e-mail: gomory@astro.sk
[2] Sterrekundig Instituut, Utrecht University, PO Box 80000, 3508 TA Utrecht, The Netherlands
[3] Max-Planck-Institut für Sonnensystemforschung, Max-Planck-Straße 2, 37191 Katlenburg-Lindau, Germany
[4] Kiepenheuer-Institut für Sonnenphysik, Schöneckstr. 6, 79104 Freiburg, Germany

Received 6 July 2005 / Accepted 17 November 2005

ABSTRACT

We analyze temporal variations in the intensities and the Doppler shifts of He I 584.33 Å (chromosphere), O V 629.73 Å (transition region), and Mg IX 368.07 Å (corona) measured in and above chromospheric network near disk center with the Coronal Diagnostic Spectrometer (CDS) onboard the Solar and Heliospheric Observatory (SOHO). There is significant correlation between the He I and O V modulations, with O V intensity leading He I intensity by 27.3 s ± 4.6 s but no significant time shift in the Doppler shift. Cross-correlation between the O V and Mg IX intensities reveals multiple maxima without correlation between their Doppler shifts. Wavelet power analysis gives evidence of intermittent chromospheric and transition-region oscillations with periodicities in the 250−450 s range and of coronal oscillations in the 110−300 s range. Wavelet phase difference analysis shows that the determined time shift between variations of the He I and O V intensities is dominated by waves with about 300 s periodicity. We interpret these results as giving evidence of compressive waves that propagate downward from the transition region to the chromosphere in the particular chromospheric network. We discuss different scenarios regarding origin and source localization of waves, and we speculate on their role in coronal heating above chromospheric network.

Key words. Sun: atmosphere – Sun: oscillations

1. Introduction

The proposed mechanisms to heat the solar corona can roughly be divided into two groups: *(i)* dissipation of magneto-acoustic waves excited in the photosphere, and *(ii)* magnetic reconnection in the corona (see e.g. the review by Narain & Ulmschneider 1996). We address these two mechanisms here for the quiet sun using ultraviolet spectrometry. Our approach is that the latter may discriminate between the two classes of mechanisms.

The first mechanism, wave heating, is thought to result from the footpoint motions imposed by convective motions on the strong-field fluxtubes that are visible as photospheric bright points concentrated in the magnetic network (Muller et al. 1994). Thus, the photospheric plasma motion continually affects magnetic field lines and excites magneto-acoustic waves. Such waves propagate upward along the magnetic field lines and transfer energy from the photosphere to the upper atmosphere where it may get dissipated after transformation of the waves to smaller spatial scales through phase mixing (Heyvaerts & Priest 1983) and/or resonant absorption (Ionson 1978; see e.g. the review by Walsh & Ireland 2003)

The second mechanism, reconnection heating, may occur from outer-atmosphere field topology changes imposed by photospheric footpoint motions (Priest 1982) and/or by field line deformations that produce small-scale reconnection events called nanoflares (Parker 1988) with a duration of a few seconds and scales below the present observational limits. However, a nanoflare should create strong stress in magnetic field lines which may propagate downward as a magnetic body wave. Hansteen et al. (1997) attributed the observed redshift of transition region emission lines to such downward propagating compressive waves. On the other hand, Peter et al. (2004) synthesized coronal line profiles from three-dimensional MHD modeling and showed that field-line braiding is a prime candidate for coronal heating in magnetically closed structures.

Determination of the dominant mechanism to heat the outer solar atmosphere in/above chromospheric network is often based on results obtained from analysis of the oscillatory behaviour (Hansteen et al. 2000; Banerjee et al. 2001) or from numerical modeling (Hansteen 1993; Wikstøl et al. 1997). Both techniques suggest the presence of the propagating waves in this part of the solar atmosphere.

In this paper we study wave modulation of ultraviolet emission lines in and above quiet chromospheric network. In particular, we employ cross-correlation and wavelet analysis of the intensities as well as the Doppler shifts of emission lines of He I (chromosphere), O V (transition region) and Mg IX (coronal) to study waves at different heights and their di-

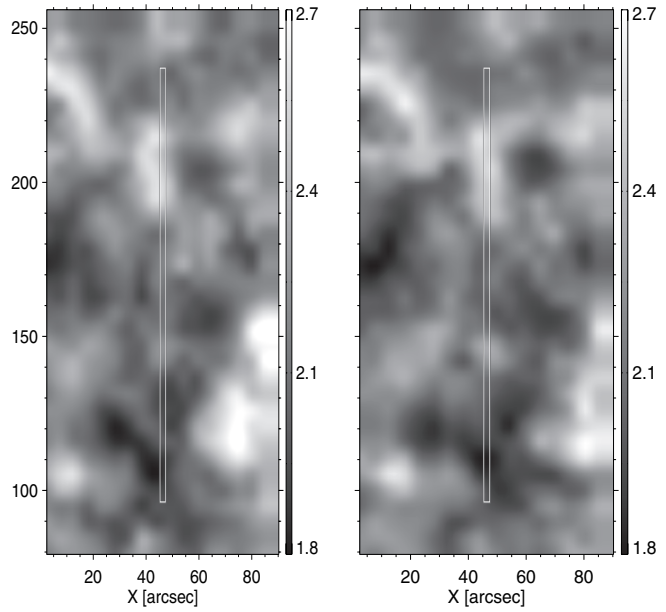

Fig. 1. CDS slit position superimposed on SOHO/EIT images in He II 304 Å ($\log T = 4.9$) at the beginning (*left*) and end (*right*) of the CDS measurements. The coordinates of the CDS slit center are $X = 46.4$ arcsec, $Y = 167.1$ arcsec relative to disk center, with Y positive to the north along meridians. Intensity in W m^{-2} sr^{-1} Å^{-1} is displayed on a logarithmic scale.

rection of propagation. Preliminary results have been reported by Gömöry et al. (2005).

2. Data and data reduction

We use data taken with the Coronal Diagnostic Spectrometer (CDS, Harrison et al. 1995) onboard the Solar and Heliospheric Observatory (SOHO, Domingo et al. 1995) in a JOP 78 (Kučera et al. 1999) from 23:25 UT until 23:53 UT on May 14, 1998. A quiet region of the solar atmosphere near disk center (Fig. 1) was observed with the normal incidence part (NIS) of CDS using the 2 arcsec wide and 141 arcsec (84 pixels) long slit in three spectral lines, namely: He I 584.33 Å ($\log T = 4.5$), O V 629.73 Å ($\log T = 5.3$) and Mg IX 368.07 Å ($\log T = 6.0$). We should remind here that the He lines have complex formation history which may be influenced by the coronal EUV radiation field (O'Shea et al. 2002). But, very recently Mauas et al. (2005) showed that even in an active region the incident coronal radiation has only very small effect on the UV lines of the He. Therefore we can assume that the detected He I radiation reflects only conditions of the upper chromosphere. A dataset of 190 spectral images with an exposure time of 5 s and cadence of 9.1 s was obtained using the "sit-and-stare" observation mode. Due to solar rotation a drift scan of 28.8 min was obtained. The final scanned area is 141 arcsec × 4.4 arcsec. As the spatial extent of chromospheric network features seen in the O V line with CDS is typically about 10 arcsec (Gallagher et al. 1998), variations of spectral line parameters shorter than one hour are likely to be local variations rather then feature drift. Moreover, Fig. 1 demonstrates that the same individual chromospheric network ($Y = 185-221$ arcsec) was observed.

Using standard CDS software[1], the raw measurements were corrected for CCD readout bias, flat-field, cosmic rays, and other instrumental effects of the CDS/NIS instrument. The measurements were then converted to physical units. For the Mg IX line, binning of 2 pixels along the slit and 5 exposures in time was performed to increase the signal-to-noise. A single Gaussian with a linear background and Poisson statistics (for pixel weighing) were used for fitting of each spectral line profile[2]. Note, that although the Mg IX 368.07 Å has a weak blend of the Mg VII (Brekke et al. 1997), which is 0.6 Å apart, the low signal-to-noise has not allowed to perform a multi-component fitting of this spectral line. The fitted data product consists of the intensities (i.e. amplitudes of the Gaussian profiles) and the Doppler shifts per spatial pixel per exposure (primary data). The wavelength scales were adjusted using the average redshift / blueshift of the transition region / coronal spectral lines of Peter & Judge (1999) and laboratory wavelengths of Macpherson & Jordan (1999). We thus obtained new reference wavelengths of our spectral lines: He I 584.330 Å, O V 629.751 Å, Mg IX 368.064 Å. The square root errors of the primary data were also calculated. Only data determined from fits with uncertainty χ^2 smaller than 10 erg^2 cm^{-4} s^{-2} sr^{-2} Å^{-2} were used.

3. Analysis

Only data of one part of the chromospheric network, henceforth called quiet network, visible in Fig. 1 on the slit between $Y = 207-213$ arcsec (i.e. four pixels along the slit) are analyzed here. These data are of the highest signal-to-noise ratio in all spectral lines and they are not influenced by eruptive events. One such event detected in the O V Doppler shift ($Y = 187-198$ arcsec) was studied in detail and identified as an explosive event (Gömöry et al. 2003).

The He I, O V and Mg IX intensities and the Doppler shifts were averaged over the four pixels covering quiet network (as specified above) for each exposure. The averaged temporal variations were then smoothed with a running mean of five time steps (Fig. 2).

Cross-correlation functions of the averaged and smoothed temporal variations of the He I, O V and Mg IX intensities as well as the Doppler shifts (Fig. 3) were calculated using the algorithm of Gömöry et al. (2004a). In this algorithm the removal of the edge pixel effect and subtraction of background trends are taken into account.

A wavelet power analysis of all temporal variations (Fig. 4) was performed using a technique developed by Torrence & Compo (1998). The Morlet wavelet (Grossman & Morlet 1984), as analyzing function, and the value of the wavenumber equal to 6 (high temporal resolution) were used for computation of the continuous wavelet power spectra. Note that wavelet transform suffers from edge effects at both ends of the time series. Therefore, all resulting periods above 500 s could

[1] http://solar.bnsc.rl.ac.uk/software/uguide/uguide.shtml

[2] http://orpheus.nascom.nasa.gov/cds/swnote/cds_swnote_47.ps

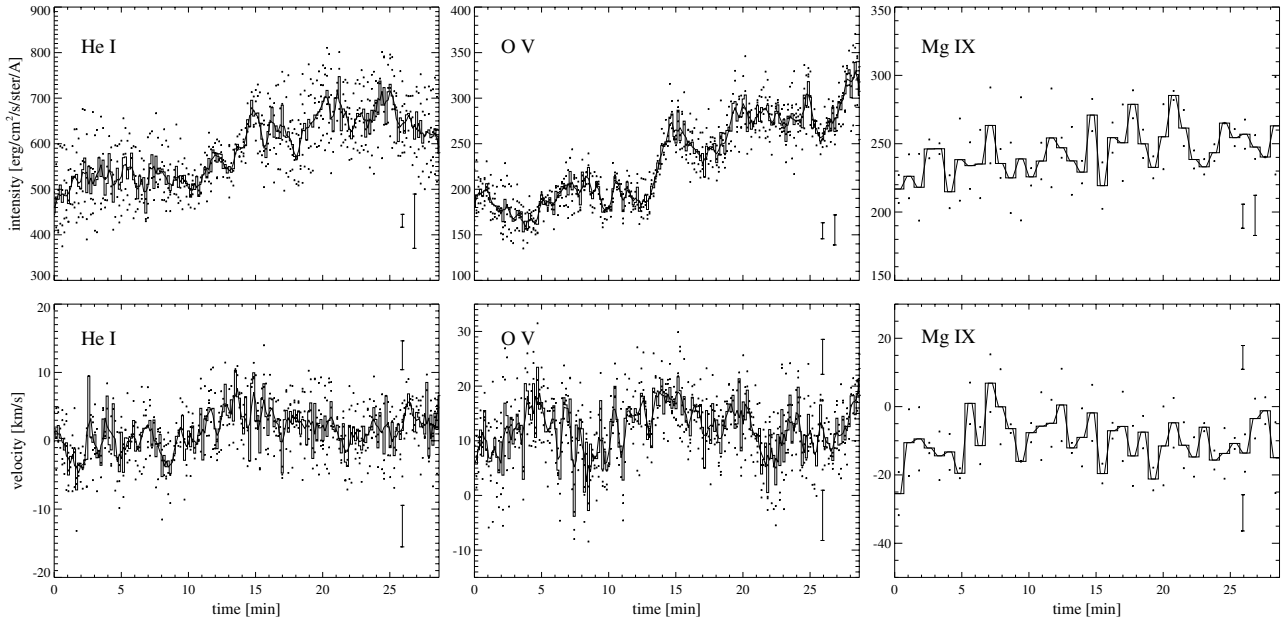

Fig. 2. Temporal variations of the He I, O V and Mg IX intensities (*upper row*) and the Doppler shifts (*lower row*). The dots show primary data (four values of four pixels along the slit for each exposure), the histograms display spatially averaged variations and the thick lines show smoothed variations. The typical square root errors of the primary data are ±14.2 erg cm^{-2} s^{-1} sr^{-1} Å^{-1}, ±8.8 erg cm^{-2} s^{-1} sr^{-1} Å^{-1} and ±9.7 erg cm^{-2} s^{-1} sr^{-1} Å^{-1} for the He I, O V and Mg IX intensities (left error bars), respectively, and ±2.1 km s^{-1}, ±3.2 km s^{-1} and ±3.5 km s^{-1} for the He I, O V and Mg IX Doppler shifts (top error bars), respectively. The mean standard deviations of the primary data from the displayed averaged temporal variations are ±59.6 erg cm^{-2} s^{-1} sr^{-1} Å^{-1}, ±16.5 erg cm^{-2} s^{-1} sr^{-1} Å^{-1} and ±17.7 erg cm^{-2} s^{-1} sr^{-1} Å^{-1} for the He I, O V and Mg IX intensities (right error bars), respectively, and ±3.1 km s^{-1}, ±4.6 km s^{-1} and ±5.8 km s^{-1} for the He I, O V and Mg IX Doppler shifts (bottom error bars), respectively. Positive values of the Doppler shifts correspond to redshift.

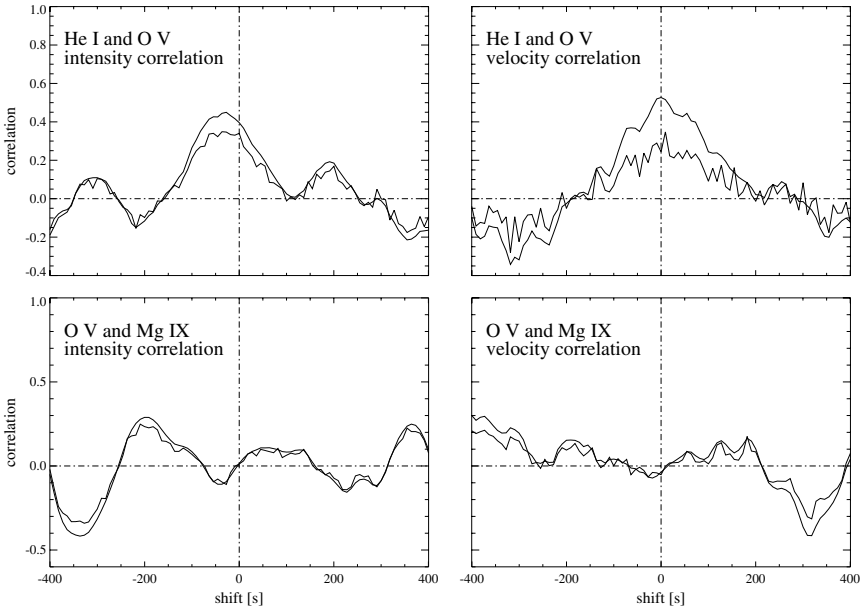

Fig. 3. Cross-correlation functions of the He I and O V intensities and the Doppler shifts (*upper row*), and of the O V and Mg IX intensities and the Doppler shifts (*lower row*). The thin lines show the cross-correlation functions of the averaged curves and the thick lines show the cross-correlation functions of the smoothed curves.

be widely affected and were not taken into account. As significance test, confidence level at 99% was calculated using a white noise background spectrum.

A wavelet phase difference (Fig. 5) was also calculated following the method of Torrence & Compo (1998) using the same wavelet and wavenumber as described above. 15% coherence exceedence level was used as significance test here (Bloomfield et al. 2004).

4. Results

4.1. Chromosphere and transition region

Figure 2 shows temporal variations of the He I and O V intensities and the Doppler shifts. The cross-correlations between the He I and O V intensities and between their Doppler shifts are shown in Fig. 3. Both cross-correlations reach values of about 0.5. The upper-left panel shows negative

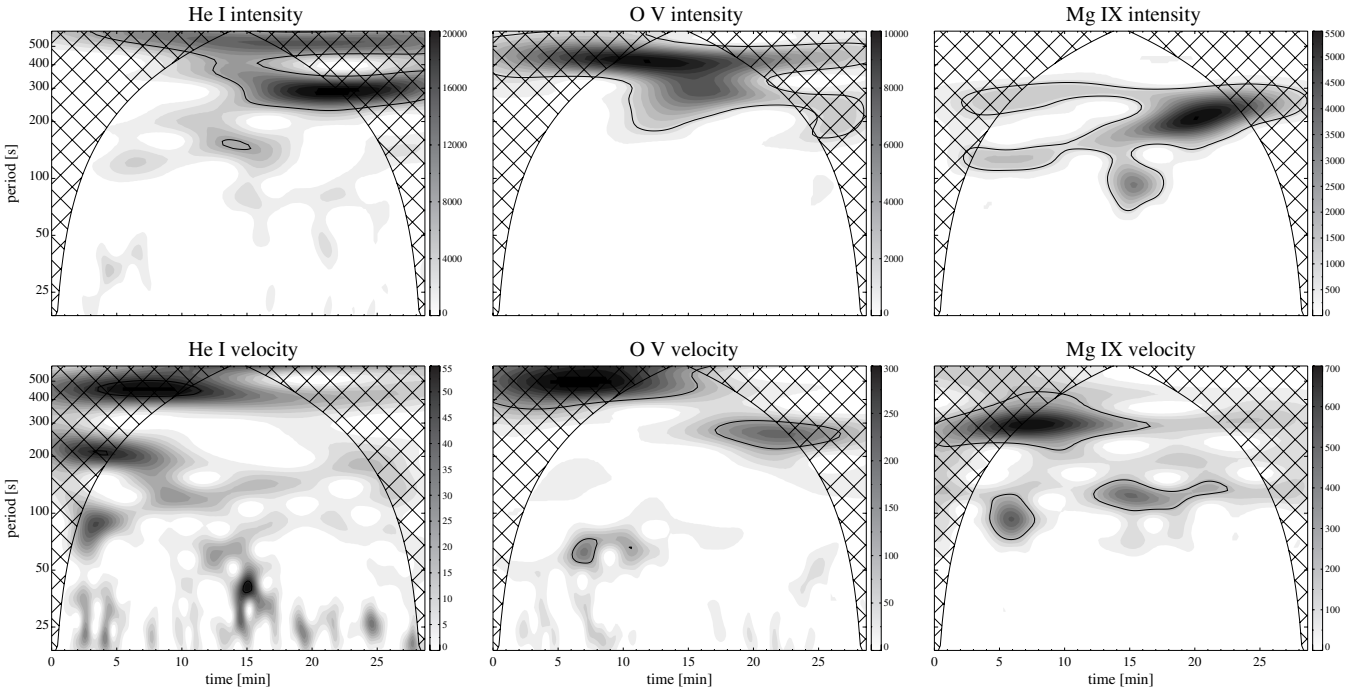

Fig. 4. Wavelet power spectra corresponding to the temporal variations of the He I , O V and Mg IX intensities (*upper row*) and the Doppler shifts (*lower row*). The gray scaling shows the power of analyzing wavelets. Contours show locations of the most relevant periods in the time series, i.e. periods with the significance more than 99%. The cross-hatched regions indicate the "cone of influence" (areas where the edge effects become important).

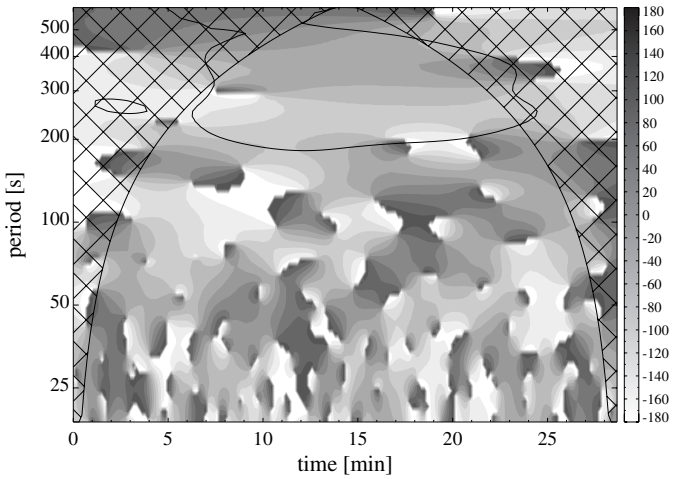

Fig. 5. Wavelet phase difference [degrees] of the He I and O V intensities. Contoured area corresponds to the 15% coherence exceedence level, while the cross-hatched area marks the "cone of influence".

time shift of –27.3 s between the He I and O V intensities. In contrast, there is no significant time shift between the He I and O V Doppler shifts. Thus, at least in some temporal subintervals, the changes in the O V intensity precede changes in the He I intensity without accompanying time shift in the Doppler shifts. Since the temporal resolution of the time series under study is 9.1 s each inferred time shift is determined with an uncertainty of ±4.55 s.

Figure 4 shows wavelet power spectra from the He I and O V intensities and from their Doppler shifts. The He I intensity modulation indicates oscillations with periodicity around 300 s, but significantly only in the time interval from 13.3 min to 28.8 min. The O V intensity reveals strong power with 250−450 s periodicity. Note that the oscillations with longer periods (around 400 s) are relevant during the whole observing sequence whereas oscillations with shorter periods (from 250 s to 300 s) occur only in the time interval from 11.6 min to 21.6 min. Moreover, no notable power with periods shorter than 200 s was found for the He I and O V intensities. The He I Doppler shift shows only oscillations with lower power which correspond to the periods around 220 s and around 450 s. These disputable periods are visible during the first 8.3 min and 15.8 min, respectively. On the other hand, it is interesting that the O V Doppler shift indicates very similar periods with the magnitude around 250 s and around 450 s but with considerably higher power. Moreover, longer periods (∼450 s) persists almost in the same time interval as the similar one detected in the He I Doppler shift. Shorter periods (∼250 s) are relevant in the second part of the observing sequence.

As the cross-correlation function of the He I and O V intensities reaches a maximum value of around 0.5 only, we used the wavelet phase difference analysis to clarify the significance of the found negative time shift between the He I and O V intensities (Fig. 5). This analysis reveals that there is relevant negative phase delay of –20° which corresponds to the time shift of –17 s between the most significant oscillations which occur simultaneously in the temporal variations of the He I and O V intensities, i.e. between oscillations with

periodicity around 300 s. Wavelet phase difference analysis of the He I and O V intensities shows phase delays also between oscillations with other periods (e.g. phase delay of –116° for the oscillations with period around 250 s). But, such results were not taken into account as these oscillations were not significant at the same time both in the temporal variations of the He I and O V intensities.

Slightly different values of the time shift obtained from the wavelet phase difference analysis and from the cross-correlation of the He I and O V intensities can be caused by the fact that whereas wavelet phase difference analysis provides temporally and frequency resolved time shifts the cross-correlation gives only averaged time shifts which are obtained as the final results from interference of all different oscillations with their particular time shifts. This also explains lower values of cross-correlation between the He I and O V intensities.

4.2. Corona

The temporal variations of the Mg IX intensity and the Doppler shift are displayed in Fig. 2. Note that binning of 2 consecutive pixels along the slit and 5 exposures in time was performed for the Mg IX line. Both temporal variations were cross-correlated with the corresponding O V curves (Fig. 3). But, only very ambiguous results were obtained from the cross-correlation function of the O V and Mg IX intensities. As this cross-correlation reaches multiple maximum (for time shifts of +200 s and −360 s) it is impossible to determine whether the changes were achieved first in the O V intensity and then in the Mg IX intensity (positive time shift) or if it was happened reversely (negative time shift). Moreover, no cross-correlation was found between the O V and Mg IX Doppler shifts.

The wavelet power spectra from the Mg IX intensity and the Doppler shift were also calculated (Fig. 4). The Mg IX intensity reveals significant power for periodicities in the range from 150 s to 300 s with the strongest peak around the period of 230 s. These oscillations are relevant mainly in the second part of the observing sequence, i.e. during the period from 15 min to 26.6 min. Note that there are also significant oscillations with periodicity around 100 s but with duration of only 3.3 min. The Mg IX Doppler shift shows relevant power for periods around 300 s which are significant for the first 15.8 min of the observations. Oscillations with periodicity around 110 s are also detected. In this case the bursty nature of the oscillations was confirmed, whereas they were relevant in the time intervals from 4.2 min to 7.5 min and from 11.6 min to 22.5 min.

5. Discussion

Several authors have studied the properties of spectral lines observed in the UV and visible part of the electromagnetic wavelength range and reported that the chromospheric plasma localized in network oscillates with a dominant period around 330 s (Kneer & von Uexküll 1993; Lites et al. 1993; Steffens et al. 1997; Judge et al. 1997; Curdt & Heinzel 1998; Krijger et al. 2001). Our analysis of the He I intensity revealed very similar dominant oscillations with a periodicity of 300 s occurring at around 15.5 min. In contrast, Doyle et al. (1998) analyzed intensity modulations of the same chromospheric spectral line (He I 584 Å) and revealed presence of dominant oscillations with considerable shorter periodicity of 200 s. But we should note that their results were not derived from the most intense regions, so the network nature of those oscillations is uncertain. In case of the He I Doppler shift we found oscillations with periodicities of 220 s and 450 s which lifetimes were at least 8.3 min and 15.8 min, respectively, but they were estimated only with low power. However, Hansteen el al. (2000) revealed that Doppler shifts of chromospheric spectral lines show strong power for periodicities in the range from 160 s to 250 s and also relevant oscillations with longer periods around 330 s and 400 s. Moreover, Banerjee et al. (2001) found that Doppler shift oscillations can extend up to values around 500 s. They also reported the intermittent nature of the chromospheric oscillations with a typical lifetime of 10 min to 15 min. Note that the discussed periods and typical lifetimes of the Doppler shift oscillations are very similar to our results, thus corroborating our findings.

Temporal variation of the O V intensity and Doppler shift discussed here showed dominant oscillations with the periodicity around 300 s and around 450 s for the intensity and oscillations with periods around 250 s and around 450 s for the Doppler shift. We also found that the lifetime of the shorter periods was approximately 10 min. Doyle et al. (1998) found that the intensities of the transition region spectral lines show oscillations with dominant periods in the range from 200 s to 500 s with the strongest power around 300 s but moreover they revealed periods with lower relevance approaching 600 s. Hansteen et al. (2000) reported relevant transition region oscillations with periodicities in a band from 100 s to 330 s with the strongest peaks around 100 s, 200 s and 330 s for intensity and 200 s for Doppler shift. Banerjee et al. (2001) pointed out that intensities of transition region spectral lines show significant power in the range from 250 s to 500 s with the strongest peaks around 280 s and 420 s, whereas the Doppler shifts do not show any significant power within this interval, but oscillate with periods close to 660 s. Moreover, they showed that the lifetime of these oscillations is approximately 20 min and can extend up to around 40 min in case of the Doppler shifts. Although we analyzed a rather short data set, the found periods as well as their times of appearance are even though in good coincidence with the previous results. Moreover, our results confirm the presence of two groups of transition region oscillations in the network, i.e. oscillations with shorter periods (~250 s) as well as with longer periods (~400 s and more).

The periods of the coronal oscillations above chromospheric network are not very well known, although there have been several attempts to determine them. Doyle et al. (1998) reported that the low signal-to-noise detected in the studied coronal line ($\log T = 6.0$) did not allow them to investigate oscillations in the corona. Banerjee et al. (2001) analyzed the same spectral line but although they found some oscillations with the periods around 100 s and 160 s the low count rates led to low reliability of these findings. Despite of lower signal-to-noise in the coronal Mg IX line, we found significant coronal oscillations with periods similar to the results of Banerjee et al. (2001). But in addition, we also revealed that these oscillations

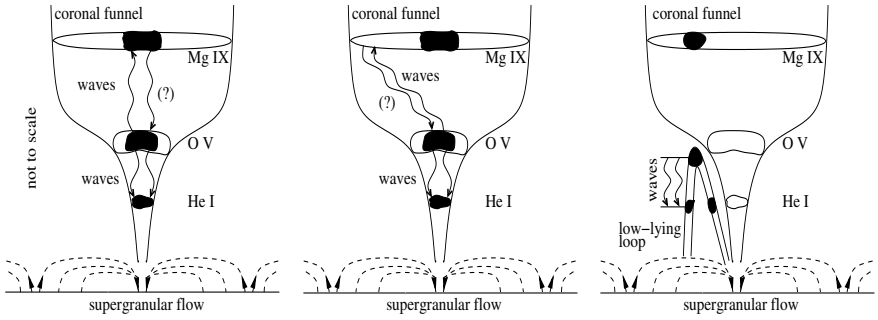

Fig. 6. Topological models of the quiet solar atmosphere above chromospheric network adopted after Gabriel (1976; *left and middle*) and after Dowdy et al. (1986; *right*) supplemented by the proposed propagating waves. The black areas correspond to the observed parts of the atmospheric layers while the white contoured areas show the whole layers where the He I, the O V and Mg IX line radiation can be generated. The wavelike arrows of different orientations describe the propagating waves.

could extend up to longer periods (~300 s). Several authors analyzed the *TRACE* measurements of the UV emissions from coronal loops and they found coronal oscillations with periods of 300 s (De Moortel et al. 2002a, 2002b; Marsh et al. 2003). We should note that the oscillations with periods of 100 s which we found in the Mg IX line intensities were present only during a very short time interval of the observing sequence, so their relevance is very uncertain.

Applying cross-correlation function to the temporal series of the He I and O V intensities we found negative time shift between them, i.e. O V intensity precedes He I intensity. The relevance of this negative time shift was confirmed by wavelet phase difference analysis of these temporal variations which moreover revealed that the obtained time shift is dominated by oscillations with 300 s periodicity. This demonstrates that the intensity changes start in the transition region and afterwards in the chromosphere. We revealed that the cross-correlation function of the Doppler shifts of these lines reaches its maximum for the time shift of 0 s. This implies simultaneous macroscopic plasma motion in the chromosphere and transition region. Following these results we can assume that the non-radiative energy had to be transfered from the transition region downward to the chromosphere without any significant bulk mass motion. Assuming a magnetic nature of the chromospheric network (Stenflo 1994; Peter 2001a, 2001b) which creates conditions for the existence of magneto-acoustic waves our results can be explained by downward propagating compressive waves taking place in this part of the solar atmosphere.

Moreover, we found that the mean spectral profiles of these lines, corrected for the instrumental profile, are dominated by non-thermal broadening. While the thermal broadening of the spectral lines is 0.018 Å for the He I and 0.034 Å for the O V, the non-thermal broadening reaches values of 0.266 Å and 0.275 Å, respectively. Instrumental line broadening was estimated by the Gaussian function with the full width at half maximum (FWHM) equal to the slit width (i.e. 2 arcsec). In order to test the reliability of obtained results we also overestimated instrumental line broadening (three times larger value of FWHM) but the resulting non-thermal broadenings remained dominant.

Wikstøl at al. (1997) simulated upward and downward propagating waves in/above chromospheric network and showed that the order of intensity changes detected in spectral lines with different formation temperatures unambiguously determines direction of the wave propagation. They also pointed out that the downward propagating waves affect profiles of the spectral lines much more strongly than upward propagating waves. In particular they showed that the spectral line broadening is much greater if the emitting plasma is influenced by downward propagating waves than by upward propagating waves. Thus, clear observational evidence of the significant non-thermal line broadening can also support the assumption of presence of downward propagating waves.

Curdt et al. (1999) studied quiet solar atmosphere in/above chromospheric network near disk center and cross-correlated the temporal variations of the Ca II K intensities with the intensities of the higher lines of the hydrogen Lyman series and Lyman continuum. They found positive time shifts and interpreted them as evidence of propagating waves that are spreading out from the chromosphere to the transition region. Summarizing their and our results we can assume that both downward as well as upward propagating waves can occur between the quiet chromospheric and transition region layers in the network at different times.

The ambiguous interpretation of the cross-correlation function of the O V and Mg IX intensities (multiple maximum) does not allow to determine if the proposed waves originate in the corona and then spread down to lower parts of the solar atmosphere or if they originate in the transition region and later affect the chromosphere and corona (Fig. 6, left). Hansteen (1993) studied perturbations of the coronal magnetic field lines (nanoflares) and reported that pure acoustic waves as well as magneto-acoustic waves excited by nanoflares can effectively propagate downward (i.e. they are not dumped). They also found that slower acoustic waves reach the transition region approximately 30 s earlier than the chromosphere what is in good agreement with determined time shift between the He I and O V intensities. Calculation of Hansteen et al. (1997) furthermore showed that these waves are hardly detectable in the Mg IX line what can explain why we have not found their clear signature in this spectral line.

Moreover, if we follow Gabriel's model of the transition region (Gabriel 1976) then it is also possible that the observed parts of the transition region and the corona were not magnetically coupled. In this case the waves could be magnetically driven from an unobserved part of the corona to the observed part of the transition region but also vice versa (Fig. 6, middle). This suggestion is supported by *TRACE* co-observations in the Fe IX 171 Å channel (Gömöry et al. 2004b) which show a much more extended area of coronal emission above chromospheric network under study. So the assumption that the waves could originate in the part of the corona unobserved by the CDS instrument is not in contradiction with our findings.

On the other hand, low cross-correlation of the O V and Mg IX intensities and no cross-correlation between their Doppler shifts could predict that the signals discussed here originated in different magnetic structures (Fig. 6, right). The multicomponent model of the chromospheric network (Dowdy et al. 1986, Peter 2001a) predicts the existence of small low-lying loops next to the magnetic funnels. Although the radiation emitted from these different structures can be in principle resolved (Peter 2001a, 2001b) the CDS spectral resolution is not high enough to achieve this goal. Following this model it can be alternatively assumed that the observed downward propagating waves occur only in low-lying loops and do not affect the corona above the particular chromospheric network.

6. Conclusion

Although we are not able to localize the original source of waves, we clearly show the presence of the downward propagating compressive waves spreading from the transition region to the chromosphere. Moreover, the time shift between the He I and O V intensities discussed here corresponds with the results determined by Hansteen (1993) for the downward propagating compressive waves excited by nanoflares in corona. This probably points to the coronal origin of the proposed waves. Following this we can state that our observational findings do not conflict with predictions derived for the reconnection heating mechanism of the outer solar atmosphere above chromospheric network.

Acknowledgements. CDS is part of SOHO, the Solar and Heliospheric Observatory, which is a mission of international cooperation between ESA and NASA. P.G., J.R. and A.K. are grateful to the Slovak grant agency VEGA for support of this work (grant No. 2/6195/6). This research is part of the European Solar Magnetism Network (EC/RTN contract HPRN-CT-2002-00313) and part of the Marie Curie Fellowship Stay at the NOVA training site (contract HPMT-CT-2001-00245). P.G. is grateful to Prof. R. J. Rutten for his comments and corrections. Wavelet software was provided by C. Torrence and G. Compo (`http://paos.colorado.edu/research/wavelets/`).

References

Banerjee, D., O'Shea, E., Doyle, J. G., & Goossens, M. 2001, A&A, 371, 1137
Bloomfield, D. S., McAteer, R. T. J., Lites, B. W., et al. 2004, ApJ, 617, 623
Brekke, P., Kjeldseth-Moe, O., Brynildsen, N., et al. 1997, Sol. Phys., 170, 163
Curdt, W., & Heinzel, P. 1998, ApJ, 503, L95
Curdt, W., Heinzel, P., Schmidt, W., et al. 1999, in Magnetic Fields and Solar Processes, ed. A. Wilson, The 9th European Meeting on Solar Physics, September 12−18, 1999, Florence, Italy, ESA SP-448, 177
De Moortel, I., Hood, A. W., Ireland, J., & Walsh, R. W. 2002a, in Solar Variability: From Core to Outer Frontiers, ed. A. Wilson, The 10th European Solar Physics Meeting, September 9−14, 2002, Prague, Czech Republic, ESA SP-506, 509
De Moortel, I., Ireland, J., Hood, A. W., & Walsh, R. W. 2002b, A&A, 387, L13
Domingo, V., Fleck, B., & Poland, A. I. 1995, Sol. Phys., 162, 1
Dowdy, J. F., Rabin, D., & Moore, R. L. 1986, Sol. Phys., 105, 35
Doyle, J. G., van den Oord, G. H. J., O'Shea, E., & Banerjee, D. 1998, Sol. Phys., 181, 51
Gabriel, A. H. 1976, Phil. Trans. Roy. Soc. London, A281, 339
Gallagher, P. T., Phillips, K. J. H., Harra-Murnion, L. K., & Keenan, F. P. 1998, A&A, 335, 733
Gömöry, P., Rybák, J., Kučera, A., Curdt, W., & Wöhl, H. 2003, Hvar Obs. Bull., 27, 67
Gömöry, P., Rybák, J., Kučera, A., Curdt, W., & Wöhl, H. 2004a, in Coronal Heating, ed. R. W. Walsh, J. Ireland, D. Danesy, & B. Fleck, SOHO 15 Conference, September 6−9, 2004, St. Andrews, Scotland, UK, ESA SP-575, 400
Gömöry, P., Rybák, J., Kučera, A., Curdt, W., & Wöhl, H. 2004b, in Waves, Oscillations and Small-scale Transient Events in the Solar Atmosphere: A Joint View from SOHO and TRACE, ed. H. Lacoste, SOHO 13 Conference, September 29−October 3, 2003, Palma de Mallorca, Balearic Islands, Spain, ESA SP-547, 303
Gömöry, P., Rybák, J., Kučera, A., Curdt, W., & Wöhl, H. 2005, Hvar Obs. Bull., 29, 71
Grossman, A., & Morlet, J. 1984, SIAM J. Math, 15, 723
Hansteen, V. H. 1993, ApJ, 402, 741
Hansteen, V. H., Maltby, P., & Malagoli, A. 1997, in Magnetic Reconnection in the Solar Atmosphere, ed. R. D. Bentley, & J. T. Mariska, Yohkoh Conference, March 20−22, 1996, Bath, ASP Conf. Ser., 111, 116
Hansteen, V. H., Betta, R., & Carlsson, M. 2000, A&A, 360, 742
Harrison, R. A., Sawyer, E. C., Carter, M. K., et al. 1995, Sol. Phys., 162, 233
Heyvaerts, J., & Priest, E. R. 1983, A&A, 117, 220
Ionson, J. A. 1978, ApJ, 226, 650
Judge, P. G., Carlsson, M., & Wilhelm., K. 1997, ApJ, 490, L195
Kneer, F., & von Uexküll, M. 1993, A&A, 274, 584
Krijger, J. M., Rutten, R. J., Lites, B. W., et al. 2001, A&A, 379, 1052
Kučera, A., Curdt, W., Fludra, A., Rybák, J., & Wöhl, H. 1999, in JOSO Annual Report 1998, ed. A. Antalová, H. Balthasar, & A. Kučera, Astronomical Institute, Slovak Academy of Sciences, Tatranská Lomnica, 149
Lites, B. W., Rutten, R. J., & Kalkofen, W. 1993, ApJ, 414, 345
Macpherson, K. P., & Jordan, C. 1999, MNRAS, 308, 510
Marsh, M. S., Walsh, R. W., De Moortel, I., & Ireland, J. 2003, A&A, 404, L37
Mauas, P. J. D., Andretta, V., Falchi, A., et al. 2005, ApJ, 619, 604
Muller, R., Roudier, Th., Vigneau, J., & Auffret, H. 1994, A&A, 283, 232
Narain, U., & Ulmschneider, P. 1996, Space Sci. Rev., 75, 453
O'Shea, E., Muglach, K., & Fleck, B. 2002, A&A, 387, 642
Parker, E. N. 1988, ApJ, 330, 474
Peter, H., & Judge, P. G. 1999, ApJ, 522, 1148
Peter, H. 2001a, A&A, 374, 1108
Peter, H. 2001b, in Solar Encounter, ed. B. Battrick, & H. Sawaya-Lacoste, First Solar Orbiter Workshop, May 14−18, 2001, Puerto de la Cruz, Tenerife, Spain, ESA SP-493, 327
Peter, H., Gudiksen, B. V., & Nordlund, Å. 2004, ApJ, 617, L85
Priest, E. R. 1982, Solar Magnetohydrodynamics (Dordrecht, Holland: D. Reidel Publishing Company)
Steffens, S., Deubner, F. L., Fleck, B., et al. 1997, in Advances in Physics of Sunspots, ed. B. Schmieder, J. C. del Toro Iniesta, & M. Vázquez, 1st Advances in Solar Physics Euroconference, ASP Conf. Ser., 118, 284
Stenflo, J. O. 1994, Solar Magnetic Fields: Polarized Radiation Diagnostics (Dordrecht, Holland: Kluwer Academic Publishers)
Torrence, C., & Compo, G. P. 1998, Bull. Amer. Meteor. Soc., 79, 61
Walsh, R. W., & Ireland, J. 2003, A&AR, 12, 1
Wikstøl, Ø., Judge, P. G., & Hansteen, V. H. 1997, ApJ, 483, 972